Diffraction Processing of Downhole Passive Monitoring Data to Image Hydrofracture Locations

Brian Fuller, Les Engelbrecht, Rich Van Dok, Marc Sterling, HiPoint Reservoir Imaging, LLC*

Summary

Seismic monitoring of hydrofracture operations can provide valuable information to guide production strategy. We present an algorithm for processing seismic fracture monitoring data. The method is more closely related to seismic reflection imaging methods such as the diffraction stack or Kirchhoff migration than the commonly used methods that use the delay time between P-wave and S-wave arrivals.

Introduction

Tight oil and gas bearing formations can contain large amounts of valuable hydrocarbon resources however low formation permeability can preclude profitable operation of production wells. Artificial permeability can be created within a reservoir however by pumping high pressure fluids into the formation in order to break the rock and form fractures. Fractures can propagate thousands of feet into the rock formation when the fluid pressure exceeds the breaking strength of the rock, thus providing a pathway for gas and fluids to migrate into the borehole and drain the reservoir. The purpose of seismic fracture monitoring is to determine the direction and distance that fractures propagate from the treatment well. Subsequent production wells can then be drilled in locations where artificially created fractures are not already draining fluids. Optimally placed wells maximize production at minimal drilling cost.

A method by which fracture locations can be estimated has been reported in multiple publications and open meetings (House, et al, 2004). The method involves using measured time delays between P-wave and S-wave seismic events generated when the fracture opens and is similar to earthquake location methods (Jeffreys and Bullen, 1940 for example). We propose an alternative fracture location technique using methods akin to diffraction stacks and Kirchhoff depth migration.

Acquisition of Downhole Fracture Monitoring Data:

Figure 1 sketches the components of a downhole seismic fracture monitoring survey. Data is typically continuously recorded over many hours with 3-component downhole geophones that should be placed to optimize the accuracy data processing results. The frequency content of fracture monitoring data varies between 200 Hz and into the kilohertz range thus the sample interval at which data is recorded should be set to accurately represent the maximum frequency present in the waveform. The number of downhole 3-component geophones used in fracture monitoring projects varies from a small number such as 4 in a single borehole with numbers greater than 40 in a single borehole becoming more common. The number of observation wells in which geophones are placed is typically only one due to practical constraints of available adjacent boreholes however some monitoring datasets have been simultaneously recorded in multiple wells.

A Common Data Processing Method:

Seismic wavefields recorded in fracture monitoring experiments differ from seismic waves in the commonly-used reflection seismic method in that the seismic source in a fracture monitoring experiment occurs at an unknown location and at an unknown time. The goal of processing downhole fracture monitoring data is to determine both the location and time of the event based on seismic events recorded in adjacent boreholes.

A common method of approximating the location of fracture formation via downhole seismic data is based on earthquake location technology. Successful implementation of the method requires the fracture to have generated a P-wave and an S-wave when the fracture opens. The data processor measures the arrival time difference between the faster P-wave and the slower S-wave seismic events. The distance of the fracture from the seismic receivers can be estimated as a function of the P-S travel time difference and P-wave and S-wave velocity fields. The direction of the fracture event relative to the receiver array is approximated by finding the geophone component rotation angles that indicate the direction from which the P-wave event energy arrived at the downhole geophones. Hence the P-S delay times and P and S velocities give the distance of the event from the seismic receivers and the 3-component energy analysis of P-wave arrivals provides the approximate direction of the event from the seismic receivers.

Significant problems are evident with practical application of this method. First, field data show that an observable P-wave/S-wave pair is not always generated when a fracture opens. In other words a P-wave may occur by itself without a following S-wave; similarly, an S-wave may occur by itself without a preceding P-wave. Thus, there is no guarantee that a P-wave/S-wave pair selected for the delay time analysis described above have a common origin at the fracture location. The pair of waves may or may not be related leading to uncertainty in the validity of event locations. A second problem with this method is that in many locations the wavefield created by rocks breaking is too complex to uniquely identify the S-wave event.

An Alternative Data Processing Method:

We have found that difficulties with the P-S delay time processing method outlined above can be mitigated by treating the first arrivals of a fracture event as having originated at a point seismic source, thus appearing as a diffraction on seismic records. By a process akin to diffraction stack or Kirchhoff depth migration the diffractions can be mapped or propagated back to their point of origin, thus showing the location at which the fracture occurred. By resolving the location of the event the time at which the event occurred is simultaneously resolved. Figure 2 is a sketch showing a two-dimensional velocity model of the earth over which a set of grid nodes have been superimposed. The grid nodes represent locations that will be tested as possible event locations in the algorithm. In practice the set of grid nodes fills a 3-dimensional space. Our processing algorithm is presented in Figure 3 in the form of “pseudo-code” as a computer algorithm is often expressed. Indented parts of the algorithm are executed within the loop immediately above the indented part of the algorithm.

The algorithm in Figure 3 is tuned to essentially stack the event signals recorded on the 3-component borehole geophones and then scale the stack by the value of semblance in a window around the predicted travel time of the wavefield. When a high-amplitude event is passed through the algorithm each grid node is tested as a possible point of origin for the observed seismic event over a range of possible times at which the event originated. The weighted stack value that results when the correct event location and event time are tested is normally distinctly larger than the surrounding grid nodes and event times. The degree to which the stack value is distinct relative to its neighbors is a measure of uncertainty in the solution.

Figure 4 shows the result of running the algorithm discussed above on continuously recorded fracture monitoring data. The algorithm requires no event picking and minimal human intervention during data processing though all events that are identified are subjected to human scrutiny as a final test of their validity.

Conclusions:

The seismic processing method presented estimates the location and time at which fractures occur during hydrofracturing operations. The method is not subject to the restriction that P-waves and S-waves must both be present in order to locate the event. Alleviation of the S-wave restriction is particularly important in projects such as the one shown here in which distinct S-waves were not present in the data thus solutions involving a P-wave/S-wave pair would have contained a high level of uncertainty.

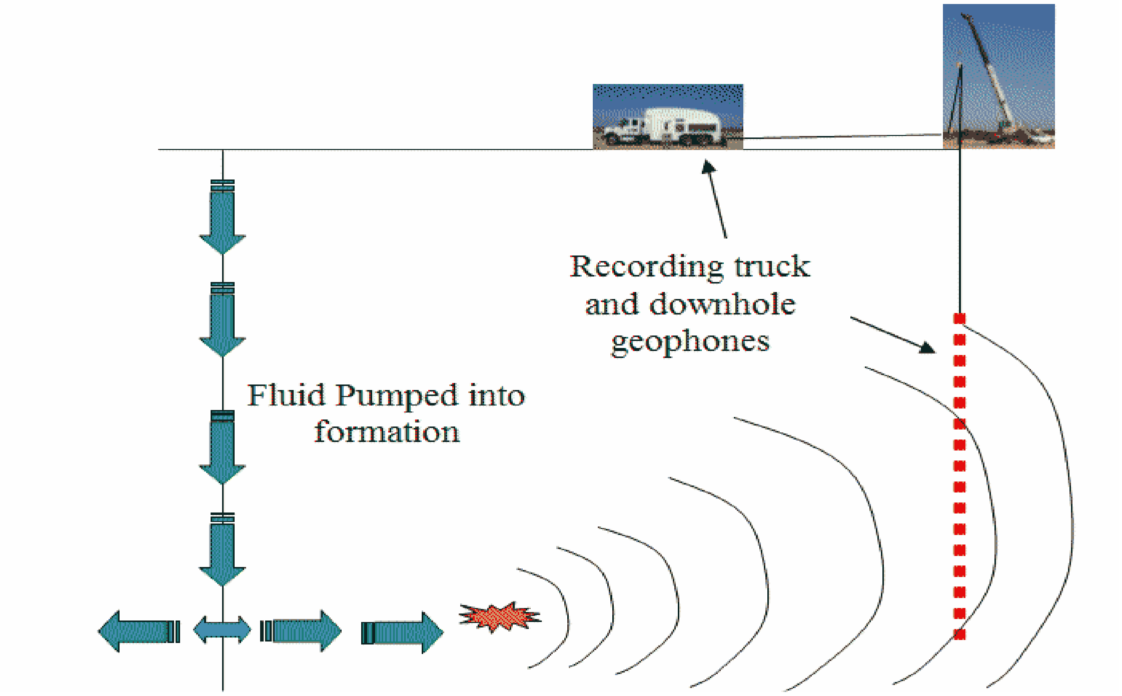

Figure 1: The components of a fracture monitoring system include a recording system at the surface and geophones in a borehole.

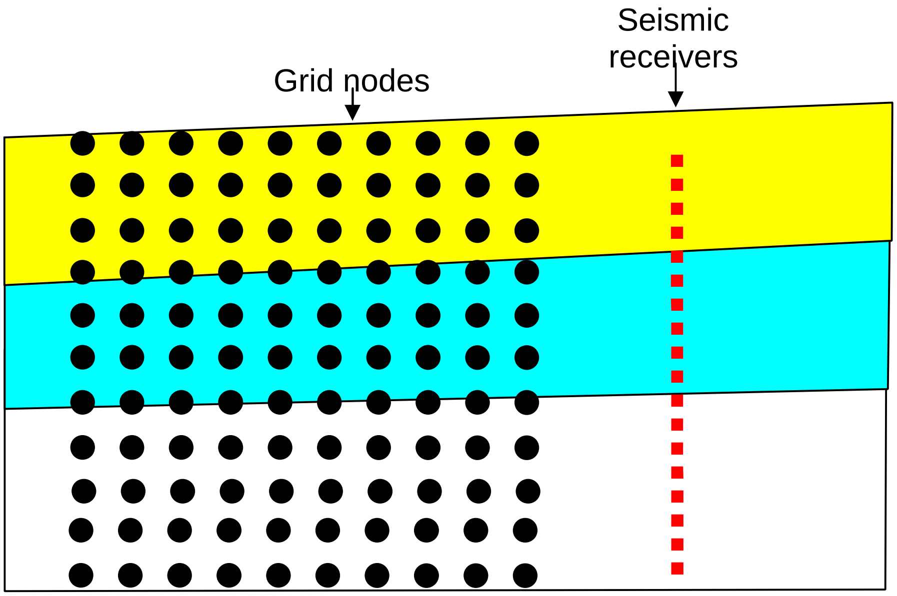

Figure 2: Grid nodes overlayed on a 2D velocity field. Each grid node is considered to be a possible location at which a fracture occurred. In practice the grid nodes fill a 3D volume for location of fracture events in space.

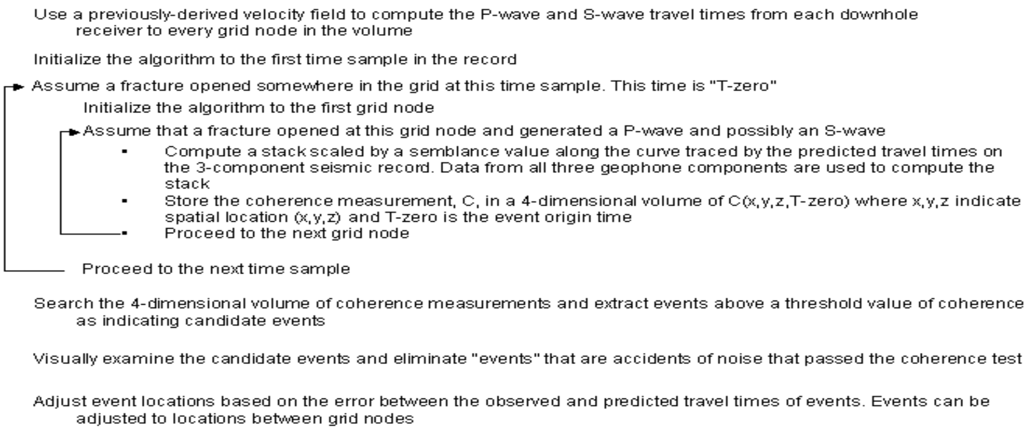

Use a previously-derived velocity field to compute the P-wave and S-wave travel times from each downhole receiver to every grid node in the volume

Initialize the algorithm to the first time sample in the record

Assume a fracture opened somewhere in the grid at this time sample. This time is "T-zero"

  Initialize the algorithm to the first grid node

  Assume that a fracture opened at this grid node and generated a P-wave and possibly an S-wave

  - Compute a stack scaled by a semblance value along the curve traced by the predicted travel times on the 3-component seismic record. Data from all three geophone components are used to compute the stack
  - Store the coherence measurement, C, in a 4-dimensional volume of C(x,y,z,T-zero) where x,y,z indicate spatial location (x,y,z) and T-zero is the event origin time
  - Proceed to the next grid node

  Proceed to the next time sample

Search the 4-dimensional volume of coherence measurements and extract events above a threshold value of coherence as indicating candidate events

Visually examine the candidate events and eliminate "events" that are accidents of noise that passed the coherence test

Adjust event locations based on the error between the observed and predicted travel times of events. Events can be adjusted to locations between grid nodes

Figure 3. Data processing algorithm for fracture monitoring data.

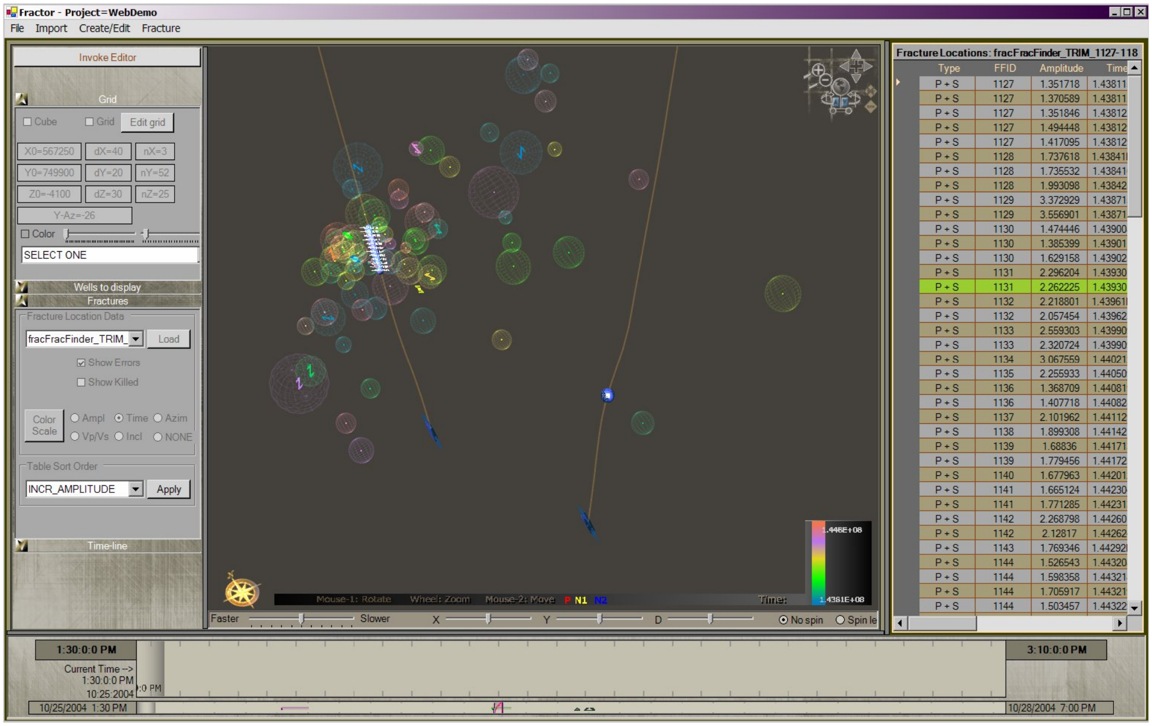

☐ Cube ☐ Grid

X0=567250 dX=40 nX=3
Y0=749900 dY=20 nY=52
Z0=-4100 dZ=30 nZ=25
Y-Az=-26

☐ Color

SELECT ONE

Fracture Location Data: fracFracFinder_TRIM_

☑ Show Errors
☐ Show Killed

○ Ampl ● Time ○ Azim
○ Vp/Vs ○ Incl ○ NONE

Table Sort Order: INCR_AMPLITUDE

● No spin ○ Spin le

1:30:0:0 PM
Current Time -->
1:30:0:0 PM
10:25:2004
10/25/2004 1:30 PM
3:10:0:0 PM
10/28/2004 7:00 PM

Fracture Locations: fracFracFinder_TRIM_1127-118

Type	FFID	Amplitude	Time
P + S	1127	1.351718	1.43811
P + S	1127	1.370589	1.43811
P + S	1127	1.351846	1.43812
P + S	1127	1.494448	1.43812
P + S	1127	1.417095	1.43812
P + S	1128	1.737618	1.43841
P + S	1128	1.735532	1.43841
P + S	1128	1.993098	1.43842
P + S	1129	3.372929	1.43871
P + S	1129	3.556901	1.43871
P + S	1130	1.474446	1.43900
P + S	1130	1.385399	1.43901
P + S	1130	1.629158	1.43902
P + S	1131	2.296204	1.43930
P + S	1131	2.262225	1.43930
P + S	1132	2.218801	1.43961
P + S	1132	2.057454	1.43962
P + S	1133	2.559303	1.43990
P + S	1133	2.320724	1.43990
P + S	1134	3.067559	1.44021
P + S	1135	2.255933	1.44050
P + S	1136	1.368709	1.44081
P + S	1136	1.407718	1.44082
P + S	1137	2.101962	1.44112
P + S	1138	1.899308	1.44142
P + S	1139	1.68836	1.44171
P + S	1139	1.779456	1.44172
P + S	1140	1.677963	1.44201
P + S	1141	1.665124	1.44230
P + S	1141	1.771285	1.44231
P + S	1142	2.268798	1.44260
P + S	1142	2.12817	1.44262
P + S	1143	1.769346	1.44292
P + S	1144	1.526543	1.44320
P + S	1144	1.598358	1.44321
P + S	1144	1.705917	1.44321
P + S	1144	1.503457	1.44322

Figure 4. Fracture event locations are shown in a 3D viewer after frature monitor seismic data are run through the algorithm discussed above.

DOI:10.1190/1.2792740

EDITED REFERENCES

Note: This reference list is a copy-edited version of the reference list submitted by the author. Reference lists for the 2007 SEG Technical Program Expanded Abstracts have been copy edited so that references provided with the online metadata for each paper will achieve a high degree of linking to cited sources that appear on the Web.

REFERENCES

House, N., B. Fuller, and J. Shemeta, 2004, Integration of surface seismic, 3D VSP, and microseismic hydraulic fracture mapping to improve gas production in a tight complex reservoir: 74th Annual International Meeting, SEG, Expanded Abstracts, 414–416.

Jeffreys, H., and K. E. Bullen, 1940, Seismological tables: British Association for the Advancement of Science.